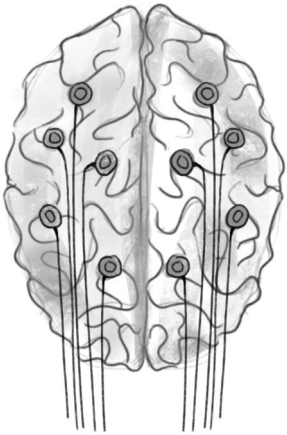

Towards real-time classification of EEG motor imagery with deep learning

Aleksandrs Baskakovs

Aarhus University

Department of Linguistics, Cognitive Science and Semiotics

Luke Ring

Aarhus University

Department of Linguistics, Cognitive Science and Semiotics

Abstract

Brain-Computer Interfaces (BCIs) have been widely employed to identify users' intention to control external objects by decoding motor imagery (MI) from an electroencephalogram (EEG). In recent years, the contribution of deep learning (DL) has had a phenomenal impact on MI-EEG-based BCI. Specifically, deep learning is highly attractive for MI-BCI as it requires little to no preprocessing, which results in a significant decrease in latency between a patient's intention and the execution of the command by the device, be it a prosthetic or a cursor. This study investigates the feasibility of using low-cost dry-electrode EEG recording to capture motor imagery for training neural networks to classify imagined right-hand fist clenches vs resting conditions and subsequent real-time online inference. This holds importance for many kinds of brain-computer interfaces, especially for people with impaired movement. The online aspect is optimized to minimize latency with a hard limit of 1 second from capture to classification. A complete end-to-end pipeline is provided, and although high levels of classification accuracy were not achieved, the framework sets up a clear path to implement rapid inference on consumer devices and suggests several future avenues to improve the quality and accuracy of results.

Introduction

Brain-Computer Interfaces

Brain-computer interfaces (BCIs) translate users' intentions via brain activity into external device commands used for interaction with the environment, applications, hardware devices, and prosthetics. The methods for measuring brain activity are usually divided into two categories: invasive and non-invasive. Invasive methods include electrocorticography (ECoG), where electrical potentials are recorded on the surface of the brain underneath the skull and microelectrode recordings, where electrodes thinner than the width of the human hair are inserted into the brain for the recording and stimulation of deeper brain structures (Schalk & Leuthardt, 2011). Brain activity can be measured non-invasively via electrical potentials on the scalp using electroencephalography (EEG) (Abiri et al., 2019), via magnetic field changes using magnetoencephalography (MEG) (Paek et al., 2020), and via metabolic processes related to brain function using functional magnetic resonance imaging (fMRI) (Sitaram et al., 2007), positron emission tomography (PET) (Nutt, 2002), and functional near-infrared spectroscopy (fNIRS) (Schalk, 2009).

In addition to degrees of invasiveness, the described sensor modalities can be distinguished by their temporal and spatial resolution. Temporal resolution is the capacity of a method to detect changes in activity over time, whereas spatial resolution is the degree to which a given method can detect changes in activity by location (Friston, 2009). In the context of BCIs, temporal resolution refers to how precisely a method can detect exactly when an event in a brain occurred, and spatial resolution refers to the precision of a method for detecting exactly where an event in a brain occurred. Additionally, the methods can be compared with respect to the degree of mobility they

afford the subject. Mobility is highly relevant in the case of brain-computer interfaces, as the usability of real-world deployments of BCI applications would heavily rely on the ability of the user to move their body freely. Table 1 illustrates how the non-invasive neuroimaging methods (EEG, MEG, fMRI, PET, and fNIRS) compare across the three dimensions.

Table 1:

Method	Temporal resolution	Spatial Resolution	Degree of mobility
EEG	High	Low	Medium
fMRI	Low	High	Low
fNIRS	Low	Medium	High
MEG	High	Medium	Low
OPM-MEG	High	Medium	High
PET	Low	High	Low

Note. *Neuroimaging methods compared against the dimensions of spatial and temporal resolution, and the degree of mobility.*

Examples of BCI implementations include, but are not limited to: brain-to-text communication via intracortical electrode recordings which decode handwriting movement attempts from a paralyzed individual into text (Willett et al., 2021), detection of drowsiness in drivers using fNIRS (Khan & Hong, 2015), and control of various external devices such as wheelchairs (Rebsamen et al., 2007), drones (Christensen et al., 2019), and robotic limbs (Lebedev & Nicolelis, 2017) using EEG.

Currently, the most practical use of BCI systems is that of enabling communication and control of devices for individuals living

with a functional impairment. However, mass adoption of such technology is hindered by the difficulty of obtaining high-quality recordings in environments outside of a lab, the processing speeds of consumer devices, and the complexity involved in building solutions that are sufficiently generalizable to be adapted to individuals or do not require expert understanding to set up (McFarland & Vaughan, 2016).

EEG-based BCIs

EEG is often considered the most practical choice for BCI applications due to its low cost, high portability, and high temporal resolution (Abiri et al., 2019). EEG measures neural activity using electrodes placed on a scalp via the flow of electric currents caused by synaptic excitations of neuronal dendrites (Olejniczak, 2006). It is often said that this is a "direct" measurement of brain activity, as opposed to fMRI or fNIRS which measure the activity via metabolic processes in the brain. EEG does not pick up the activity of individual neurons, but rather a synchronous activity of millions of neurons that have similar spatial locations. The type of neurons that produce the most EEG signals are pyramidal neurons, due to their alignment and tendency to fire together (Kirschstein & Köhling, 2009). The inability to pick up signals from individual or smaller numbers of neurons is one of the reasons for the weaker spatial resolution of EEG. Another reason for poor spatial resolution is that EEG records activity from the outer layer of the cerebrum, the cerebral cortex, and thus does not have access to deeper brain structures. Signals captured by EEG only account for around 5% of brain activity (Ball et al., 2009). However, given that EEG is able to directly sample regional brain activity at rates of 1 000 Hz or greater, it provides a high level of temporal resolution. While activity in the deeper brain structures is beyond the reach of an EEG device, the signals in the areas such as the

primary motor cortex, primary sensory cortex, temporal lobe, or occipital lobe can be reliably detected and utilized for control of external devices (Guger et al., 2000).

The use of signals found in the cortical brain areas are often referred to as "paradigms" (Abiri et al., 2019), with each paradigm having an established protocol for the development of a BCI application. The EEG is first collected while the subject repetitively performs a specific task related to the paradigm being investigated (e.g., visual or imagery task). Typically, data is then preprocessed to improve the signal-to-noise ratio and remove invalid trials, and is also used for training and validation of the decoder. Finally, the subject can use the BCI system by performing the task again, where the BCI system translates the neural signal into commands for virtual objects or external prosthetics (Abiri et al., 2019). Figure 1 illustrates a typical EEG BCI protocol. The most common EEG-BCI paradigms are motor imagery (MI) paradigms and external stimulation paradigms.

EEG-BCI paradigms

The external stimulation paradigm is based around the purposeful

Figure 1:

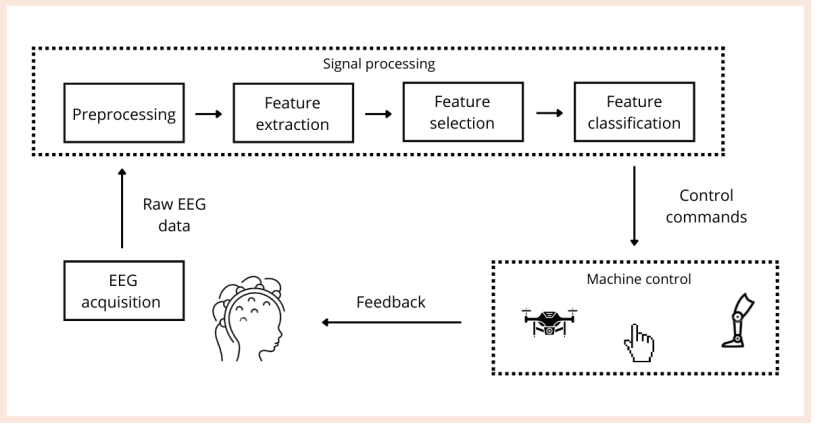

Note. *A block diagram for a general BCI system*

modulation of brain activity using outside signals - visual, auditory (Shangkai Gao et al., 2014), or somatosensory (Yao et al., 2017). For example, one of the more widely implemented BCI-enabled communication interfaces is a P300 Speller. P300 is an event-related potential, evoked in response to an external stimulus. P300 is thought to reflect the contextual meaningfulness of the stimulus for the subject. It is characterized by a large positive deflection peaking at approximately 300 ms after the presentation of the stimulus (Fabiani et al., 1987). Farwell and Donchin (1988) were the first to describe a reliable BCI communication system utilizing the P300 signal, called P300 Speller. The system presents a 6x6 grid with a character occupying each cell. The subject focuses their attention on the character they intend to spell, while each row and column of the matrix is highlighted in a random sequence (Figure 1.1). Whenever the highlighted row and column intersect at the subject's character of choice, a P300 response is elicited. A decoder is then able to spot the signal, recognize at which intersected character it was elicited and infer the subjects' character of choice. One patient with late-stage ALS has used the device for 4 to 6 hours a day for typing emails and other applications and has reported the P300 speller as superior to his eye-gaze-based system (Vaughan et al., 2006).

Another paradigm that makes use of external stimuli for the selection of commands is called a steady-state visual evoked potential or SSVEP (Vialatte et al., 2010). In this paradigm, multiple stimuli (each of which represents a command and can be visual, auditory, or somatosensory) are presented to the participant, each at a different frequency, with frequencies varying from low (1–5 Hz) to high (75–100 Hz). When a subject focuses their attention on a particular stimulus (e.g., a flickering light) EEG frequency observed over the visual areas of the brain is reliably correlated with the frequency of the re-

Figure 1.1:

Note. *The letter grid used for a typical P300 speller-based BCI. A row or column flashes for around 100 ms every 200 ms. The participant focuses his attention on one of the letters (for example, letter "D") whilst wearing an EEG cap. Whenever the row or column containing flashes (in this case, row 1 or column 4), a P300 response is elicited. The first row or the fourth column must flash multiple times (eliciting P300 response multiple times) in order for the decoder to confidently classify "D" as the participant's letter of choice. (Figure reprinted from Krusienski et al. (2008)).*

spective stimulus (Kuś et al., 2013) (Figure 1.2). Decoding which command the subject is trying to select becomes possible by matching the EEG activity pattern to the frequency of the stimulus representing the command. SSVEP is advantageous because it does not require training, can be classified more reliably than event-related potentials, and benefits from more commands due to the range of frequencies for use (Abiri et al., 2019). Applications include controlling lower limb exoskeleton (Kwak et al., 2015), orthosis (Pfurtscheller et al., 2010), and locked-in syndrome (Hwang et al., 2017).

Figure 1.2:

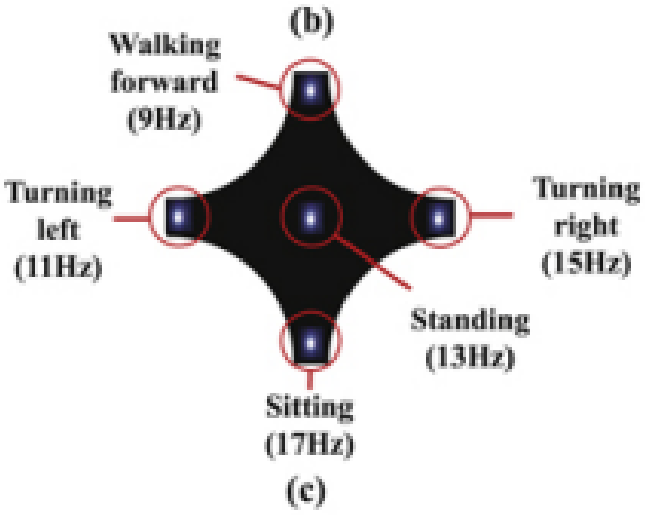

Note. *An example of a visual SSVEP interface panel used for the control of the exoskeleton from Kwak et al. (2015). Each of the white dots is an LED flickering at a specific frequency and represents a particular command. The subject focuses his attention on one of the lights while wearing an EEG cap, the activity recorded in the visual cortex is then correlated with the frequency of each of the lights. The command whose respective flickering frequency correlates the most with the activity is then classified as being the intent of the subject.*

Since external stimulation paradigms heavily rely on constant and repetitive presentation of stimuli to the subject, subjects may experience fatigue and may generally find their use difficult for long periods of time (Chang et al., 2014).

Motor imagery paradigms, on the other hand, do not rely on external stimuli, but rather on the wilful, internal modulation of neural activity. Using MI provides a unique way of interacting with hardware or software that has the potential to feel natural and relevant to the task being performed as well as being distinct from natural environmental stimuli (such as noises, flickering lights, etc.).

Motor Imagery

Motor imagery is a mental process of kinesthetically imagining movements without the respective physical movement occurring (Lotze & Halsband, 2006). One way to discern MI from visual imagery is to determine the "point of view" of the subject of the imaginal experience. On the one hand, mental images can be experienced from a third-person perspective, with the subject acting as a "spectator", watching themselves perform an action. One illustrative example is the sport of climbing, where it is commonplace for individuals to imagine an avatar ascending a specific route. On the other hand, mental images can be experienced from a first-person perspective, a process involving mostly a kinesthetic representation of the movement, during which the subject feels as if they were executing the movement. This type of imagery requires representing the process of an action being executed (Jeannerod, 1995). Kinesthetic motor imagery can be experienced by remembering and/or preparing for a set of precise movements, for example a drummer preparing to play a specific, highly technical part of a musical piece. Motor imagery falls under the type of kinesthetic imagery (Stinear et al., 2006).

Motor imagery gained its prominence as a research area due to its relevance in motor learning—the process of acquiring or strengthening a skill through repetitive practice (Newell, 1991). During repetitive practice, the subject engages neural networks responsible for the movement over and over again, strengthening the connections between the neurons through the process called Hebbian learning (Hebb, 1949), or as its famous tenet goes: "Neurons that fire together—wire together." Hebbian learning in the brain as a physical process is primarily facilitated by two neural mechanisms: long-term potentiation (LTP) (Bliss & Lømo, 1973) and long-term depression (LTD) (Artola et al., 1990). LTP and LTD influence the extent to

which activity in a sending neuron leads to activation of a receiving neuron, by influencing the efficacy of synapses or junctions between neurons. LTP is a long-lasting potentiation (strengthening) of synaptic efficacy, while LTD is a long-lasting depression (weaking) of synaptic efficacy.

Whilst physical practice is most vital for the acquisition and consolidation of new motor skills (Robertson et al., 2004), motor imagery is a well-assessed complementary practice for motor learning (Schuster et al., 2011). The rationale is that imaginary movement potentiates the activation of the sensorimotor system which leads to strengthening of neuronal connections (Kraeutner et al., 2014; Pfurtscheller & Neuper, 1997). MI is used for motor learning in both healthy populations (Dickstein & Deutsch, 2007) and for motor rehabilitation in patients (Malouin et al., 2013). This willful generation of activity in the sensorimotor cortex by performing imaginary movements is the foundation of the motor imagery paradigm in BCIs.

In the sensorimotor rhythms (SMR) paradigm, a subject imagines kinesthetic movements of body parts such as the hands, the legs, the fingers, the feet, the legs, the arms, or the tongue. Imagined movement causes event-related desynchronization (ERD) and its opposite, event-related synchronization (ERS), which is observed during relaxation. ERS and ERD phenomena are found mostly in Alpha (or mu, as it is often referred to in the context of imaging sensorimotor cortex) (8–12 Hz) and Beta (16–24 Hz) frequency bands (Pfurtscheller, 2000, p. 26). Upon the imagination of a movement, a power reduction (ERS) can be observed in the mu/beta , and a rise back in power (ERS) when the movement ceases. As with physical movements, the imaginary movements in the motor imagery paradigm are unilateral, due the location and size of neural regions responsible for specific movements differing, which leads to different signal characteristics,

thus making it possible to distinguish MI for left- and right-hand movements. When a movement of a unilateral limb is imagined, the recorded activity at the contralateral side of the motor-sensory cortex increases, while the activity at the ipsilateral side does not display an increase in activity. This contrast between location-specific signals as well as contextual EEG activity is able to be leveraged for successful classification of the user's intent.

BCI systems within the motor imagery paradigm make use of ERD/ERS events for an external application. Apart from allowing individuals with impaired function to control, for example, external limbs (Barsotti et al., 2015) or moving a wheelchair (Reshmi & Amal, 2013), MI-based BCIs are also often used for the purposes of neurorehabilitation (Pichiorri & Mattia, 2020).

Classification Approaches

Traditional signal processing approaches

EEG has a low signal-to-noise ratio due to the electrodes measuring brain activity at a microvolt level. This high sensitivity means that along with cortical brain activity, EEG recordings capture many biological processes including eye blinks, heartbeat, muscle movements, and respiration. The electrodes are also prone to interference caused by electronic equipment, including the recording equipment itself and proximity to electromagnetic fields like those generated electricity supply lines. In addition, there are cross-channel correlations and subject-specific patterns of activity (Altaheri et al., 2021). Hence, adequate classification of imagery movements strongly depends on the processing pipeline of raw EEG data, namely: preprocessing, feature extraction, feature selection, and feature classification (Khosla et al., 2020).

Usual preprocessing techniques include: notch (bandstop) filter-

ing to remove power line noise at 50 or 60 Hz (region specific); high-pass filtering for the removal of baseline drift; low-pass filtering to smooth the signal; downsampling the data for quicker computation and reduced memory storage; selection of specific electrodes dependent on the performed task; referencing from specific electrodes or the signal average from all electrodes; and band-pass filtering to select frequency range(s) of interest.

Following preprocessing, EEG data go through feature extraction, feature selection and finally, feature classification where a prediction of the intended movement occurs. Feature extraction is a stage where meaningful information is extracted from the neural data. It is often achieved using time-frequency approaches—due to the non-stationary nature of EEG signals—and further improved via spatial approaches that identify and weight channels with the highest signal-to-noise ratio. The returned feature sets are of high dimensionality, and statistical techniques such as Principal Component Analysis (PCA) (Abdi & Williams, 2010) and Independent Component Analysis (ICA) (Stone, 2002) are used for dimensionality reduction and feature selection.

Often, multiple techniques are used for each phase of extraction, selection, and classification of EEG signals (Kevric & Subasi, 2017). While high-performing, if these techniques were employed for applications requiring time-critical classification, the recurring complex computations performed on the data would introduce prohibitively high latency. Additionally, they would require expert assistance to calibrate the decoder, as MI EEG data are prone to high subject specific variance (Zhang et al., 2021), which also contributes to the problem of achieving a generalizable or, at least, easy to calibrate classifier for MI EEG signals. Thus, the classical signal processing approaches are an obstacle for achieving an easily deployable BCI system that is

able to perform accurate predictions of users intent in real-time.

Machine learning

Neural networks have been shown to achieve "end-to-end learning" by learning complicated and latent features from large amounts of data (Bojarski et al., 2016), bypassing the need for manual feature extraction, selection, and preprocessing. The promise of feeding raw data directly into the neural network without intensive signal preprocessing opens up both the latency and calibration bottlenecks for real-time BCI use (Craik et al., 2019). Specifically, convolutional neural networks (CNNs) have become very popular due in part to their success in image classification (Krizhevsky et al., 2012). Naturally, the high dimensionality EEG data has been tackled with deep learning, notably for previously mentioned visual-evoked responses (Cecotti & Graser, 2010), Alzheimer's classification (Morabito et al., 2016), depression (Acharya et al., 2018), epilepsy prediction (Hussein et al., 2019), and most relevantly, motor imagery classification (An et al., 2014; Tabar & Halici, 2017).

Following the promise of end-to-end learning, deep learning for motor imagery has experienced a rapid growth since 2017 (Altaheri et al., 2021). Since then, multiple approaches regarding preprocessing (or lack of it), input formulation, deep learning architectures, and performance evaluation have been tried. Preprocessing for MI EEG classification usually consists of selecting channels that contain the most distinct MI features and subsequent band-pass filtering. More than 79% of the studies reviewed by Altaheri et al. (2021), used all EEG channels. However, most of these studies were not oriented on online classification, where reduction of the volume of incoming data, process complexity, and computational time is a significant consideration. Over 91% of the studies reviewed in the aforementioned paper used a band-pass filter on the data to select for frequencies

where the ERD/ERS events are observed, notably the mu (8–12 Hz) and Beta (18–26 Hz) frequency bands. The band-pass filter also effectively removes the power line noise (50 Hz) from the data.

Input formulation largely depends on the architecture of the neural network and is usually one of the following four: raw signal values, spectral images, topological maps, or extracted features. The neural network is then trained on this input and judged by its ability to correctly discern the class of the input data, which could be a binary outcome or a multi-class prediction. Classification performance of a model is usually validated by using either the hold-out approach—where a portion of the data that is not included in training is used to validate predictions—or the cross-validation approach which repeatedly splits the data in different ways for training and validation. The exact method of splitting and validating data varies by the type of cross-validation. Trained models are then selected based on a specific performance metric such as maximizing accuracy or minimizing the outcome of a loss function. The selected model can then be used on novel data for inference, meaning it is able to predict the class of data outside the original dataset. Machine learning architectures arepromising contenders as a method for effective and process-efficient classification of motor imagery signals.

Present study

Whilst many have reported high-performing MI-EEG BCIs, these systems are confined to carefully controlled, noise-free, artificial environments, and are heavily dependent on expensive research-appropriate systems that require expert preparation and configuration (McCrimmon et al., 2016). Moreover, the classification is usually applied on the complete period of performing the motor imagery movement during the experimental protocol, which ranges around four seconds. In a real-time scenario, this would result in a minimum

latency of four seconds for the user, seriously inhibiting the usability of the BCI system for general tasks and making time-sensitive interactions impossible. For MI-EEG BCIs to reach a sufficient degree of practicality for everyday use, they need to be easy to set up, low-cost, robust, and most importantly, low-latency.

The main contribution of this study is the use and subsequent examination of a lightweight convolutional neural network for the real-time classification of EEG data with sub-second latency. Moreover, the EEG data is acquired in a naturalistic, interference-prone setting, using a low-cost, dry-electrode EEG device, which sheds further light on the accuracy and reliability of the BCI system for real-world applications.

Methods

Participants

Two male volunteers (both right-handed, M = 30.0, SD = 5.0 years) participated in the experiment and gave their informed consent.

Hardware and Software

Neural activity was recorded using a low-cost, open-source/open-hardware EEG device Ultracortex Mark IV Headset[1](OpenBCI, Inc., USA) with dry electrodes, connected to the OpenBCI Cyton and Daisy biosensing boards (OpenBCI, Inc., USA). The cap followed a 10–20 international electrode placement scheme. Fifteen electrodes covering the whole head were selected (Fp1, Fp2, F3, F4, F7, F8, T7, C3, C4, P3, P4, P7, P8, O1, O2). EMG monitoring was performed using three Skintact F301 foam solid gel electrodes (two signal electrodes and one ground) plugged into the OpenBCI Daisy board. EEG Reference and ground electrodes were placed at the left and right ear lobes. Figure 2 illustrates the placement of both EEG and EMG electrodes.

Offline Raw EEG and EMG data were acquired at a sample rate of 1000 Hz via a microSD-card plugged directly into the Cyton board using a custom-built Python interface[2] using the BrainFlow API[3]. The custom interface was required to send low level commands to the board and configure pin settings for the EMG signal and grounding and in addition, a modified Cyton firmware[4] was required to fix an issue with capturing data above 250 Hz.

Figure 2:

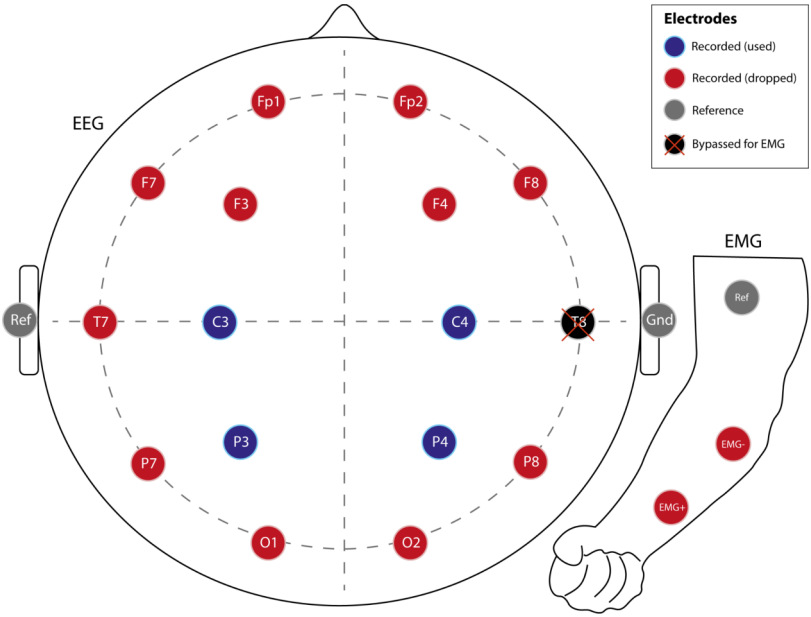

Note. *Graphic representation of the EEG and EMG electrode placement on the scalp and arm, as well as their use in classification.*

[1] https://docs.openbci.com/AddOns/Headwear/MarkIV/

[2] https://github.com/zeyus/OpenBCI_Cyton_Library

[3] https://github.com/brainflow-dev/brainflow

[4] https://github.com/zeyus/BrainflowCytonEEGWrapper

[5] https://github.com/zeyus/CogNeuroExam

[6] https://github.com/onnx/onnx

Source code for the experiment, data collection, offline analysis, model training, and online classification is available on GitHub.[5]

Online classification with sub-second latency

Model training took place on an NVIDIA GTX1070 GPU with CUDA 11.6, CUDNN v8.4.0.27, and PyTorch 1.12.0.dev20220507+cu116. After model training, the model's weights were frozen and exported in Open Neural Network Exchange (ONNX) format6, subsequently the pre-trained model was loaded into a CPU-bound instance of the ONNX Runtime (ONNX Runtime developers, 2021) and real-time streaming EEG and EMG data were collected via the Cyton USB/Bluetooth dongle using the custom interface at a sample rate of 250 Hz. Data from non-selected channels were dropped, and the remaining data were resampled and sent to the model for inference Figure 3.

Stimuli

The python package PsychoPy (Peirce et al., 2019) was used to present the stimuli to the participants. The task was to perform imaginary movements of clenching the right hand or resting. Visual cues were presented to the participant before the beginning of a new trial to ensure attention to the task. A purple arrow pointing to the right was used as a visual cue to indicate that the participant should imagine clenching their right hand, a purple arrow pointing upwards was used as a visual cue to indicate that the participant should rest, simply focusing their gaze on the arrow.

Trials and Experimental Protocol

Experimental protocol was largely adapted from Ma et al. (2020). Each trial of the experiment began with a white circle (t = -3 s) indicating the start of the trial, followed by a red circle 2 seconds later (t

Figure 3:

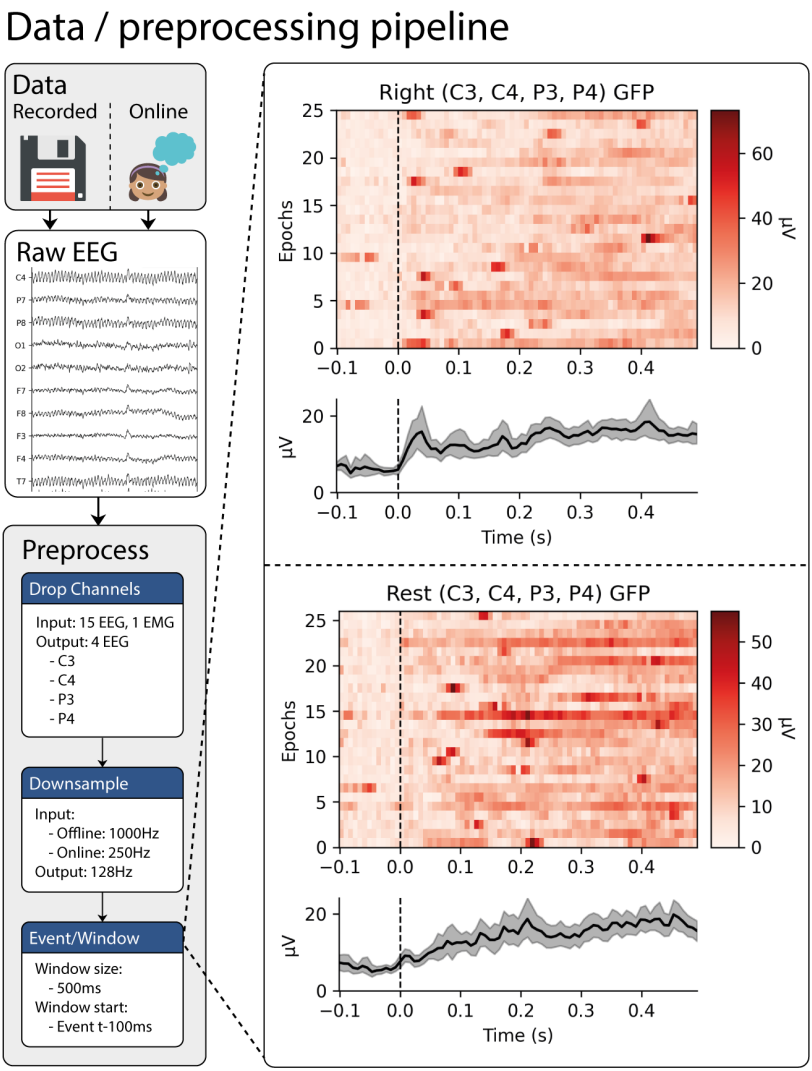

Note. *Outline of data acquisition and preprocessing pipeline.*

= -1 s), alerting the user about the upcoming stimuli onset. At t = 0 s, either the right or upward pointing arrow was presented indicating the requirement to either clench the right hand or to rest, for the duration of 4 seconds. The participants were told to perform the imaginary movement until the arrow disappeared from the screen. The

importance of imagining single, continuous movement for the total duration of 4 seconds was stressed to the participants. At the end of the trial, a short break of 1 second followed. A schematic representation of the experimental protocol can be seen in Figure 4. The session lasted until 30 trials of each of the 3 tasks were completed, which was approximately 12 minutes. 3 sessions for Subject #1 and 4 sessions for Subject #2 were recorded over multiple days.

Procedure

The participants were seated in a comfortable chair and instructed about the protocol. The importance of performing a kinesthetic imaginary movement was stressed. To avoid motion-related artifacts, the participants were asked to keep any type of movements while going through the experiment to a minimum.

Following the instructions, the EMG sensors were placed on the participants arm, namely two sensors on the inner left side of the right forearm (flexor digitorum superficialis) and one ground sensor on the right biceps (biceps brachii). The EMG electrode locations were gelled before the placement of the sensors. The dry-electrode

Figure 4:

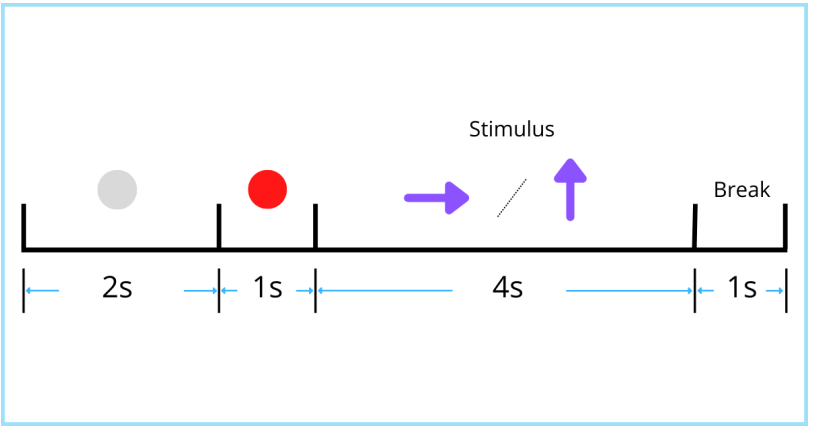

Note. *Schematic representation of the experimental protocol.*

EEG cap was placed on the participants head with the Cz electrode socket placed on the vertex of the head. Clip electrodes were used for the reference and ground electrodes, placed on ear lobes, which were cleaned with alcohol and gelled. A visual inspection of the quality of the EEG signals was done using the OpenBCI GUI. If any of the channels were shown to capture the signal poorly, the electrodes corresponding to those channels were gently turned until the quality of the signal was acceptable. Throughout the whole mounting procedure, the participants were repetitively asked whether they experienced any significant discomfort in relation to the procedure.

Data Pre-Processing

Assessment of muscle activity during trials

EMG activity was recorded along with EEG to monitor the amount of activity exhibited by the flexor digitorum superficialis muscle which is used for fist-clenching. Four prior experimental sessions (two per subject) were conducted which contained a physical fist-clench condition to compare the EMG signal of intentional physical movements with potential sub-activation levels of imagined movements. Visual inspection of EMG data from MI trials indicated that muscle activity was much weaker in imaginary movement trials (Figure 5).

Channel selection

Data from electrodes covering the sensorimotor cortex, namely, C3, C4, P3, and P4 were selected for the purposes of classification of motor imagery movements. These channels were deemed most important in capturing event related desynchronization/event-related synchronization phenomena discussed previously, via the visual inspection of the recordings. Figure 6 below illustrates average activity from C3, C4, P3, and P4 channels during rest vs. right hand condi-

tions for one participant during one of the recording sessions. The difference in activity can be distinguished most clearly in the two plots for the C3 channel, which is expected as the C3 channel covers the area of the sensorimotor cortex responsible for the movement of the right hand.

As previously noted, over 79% of studies reviewed by Hoodis used data from all electrodes for classification. However, multiple studies have achieved good accuracy using eight channels or less (Lun et al., 2020; Yang et al., 2020; Yohanandan et al., 2018). As this study heavily emphasizes the importance of sub-second latency in classifying motor imagery movements, only the essential channels are used to minimize the amount of data required for online processing. Figure 2 illustrates the placement of EEG electrodes, as well as the placement of EMG sensors mentioned above.

Band-pass filters

EEG preprocessing pipeline for MI classification often involves frequency filtering with a bandpass from 8–32 Hz or similar, the upper passband limit removes line noise from single-phase AC electricity (50 Hz or 60 Hz depending on region) and the lower passband limit helps reduce signal drifts which can be caused by changes in subject skin conductivity. Although, there is research suggesting that there is loss of relevant signal in cases of high pass (lower passband) values above 0.1 Hz (Tanner et al., 2015). In many cases, filtering can improve the signal-to-noise ratio, though the process itself can also introduce artifacts such as passband ripple, and thus there are many different approaches to identifying the important aspects of a signal, including signal decomposition methods like independent component analysis (ICA) or ML. In the case of MI classification, bandpass filtering narrows the data to the frequency where the ERD/ERS signal is observed most saliently. However, as EEGNet—which the neu-

Figure 5:

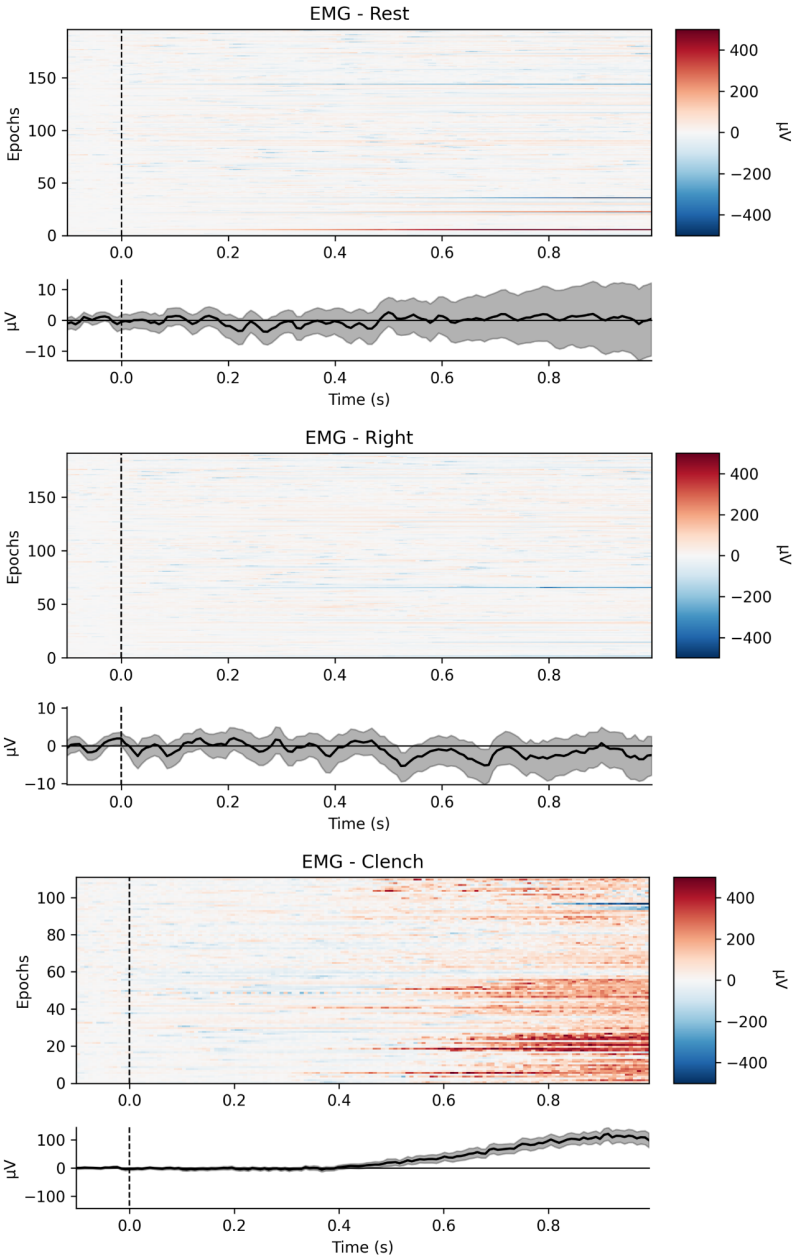

Note. *Visualization of EMG data for resting, right MI, and right hand clench trials, note the clear increase in activity and scale of the signal in the clench trials.*

Figure 6:

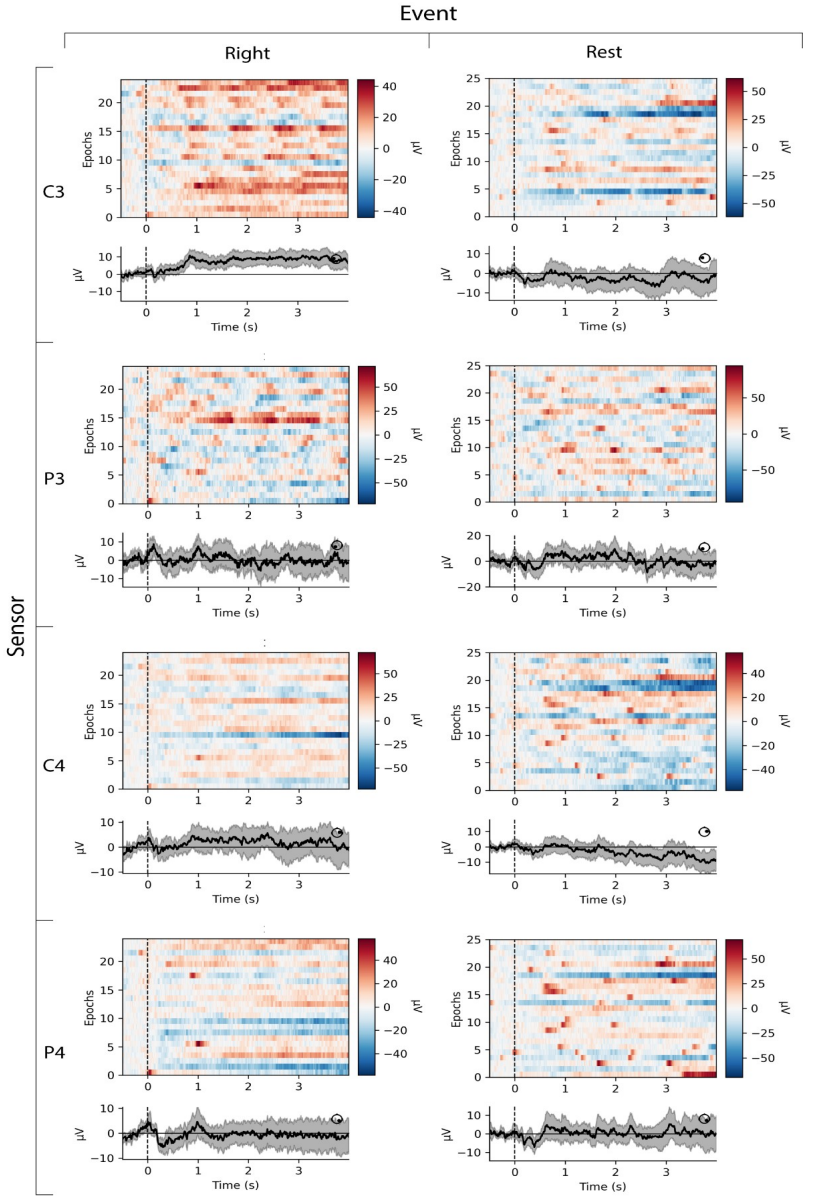

Note. *Two MI events averaged across all trials for one session of one participant as displayed by the four sensors (C3, C4, P3, P4) used in the training of the neural network.*

ral network proposed below is based on—includes temporal and spatial filters, no frequency filters are applied to the EEG data. Moreover, for real-time, online classification, any frequency-based signal filtering is severely limited by the window size of the data that is being classified, and in our case, the upper window limit of 0.795 s (□101 samples at 128 Hz) makes the introduction of artifacts extremely likely. Reducing the amount of preprocessing also has the important effect of increasing the processing speed of classification.

Neural network architecture

A multi-layered Convolutional Neural Network (CNN) architecture (Figure 7) was implemented based on EEGNet (Lawhern et al., 2018) from a modified version of DN3[7] (Kostas & Rudzicz, 2020b, p. 3). All model fitting was performed with Stochastic Gradient Descent (SGD) optimization with momentum, minimizing the two-category cross-entropy loss (Figure 8). A wide variation in hyperparameters were tried to find the optimal values for both within-subject and between-subject models, and while certain parameters such as increasing the number of temporal and spatial filters had a significant effect on increasing training accuracy, this was likely due to overfitting as the validation accuracy did not improve, Table 2 lists the hyperparameters used for the best performing model. Due to EEGNet's application of temporal and spatial filters to the EEG data, we found that the application of various preprocessing techniques (such as windowed FIR bandpass, notch filtering, and average signal subtraction) did not significantly improve classification accuracy. Additionally, strided EEGNet, BENDR (Kostas et al., 2021), and TIDNet (Kostas & Rudzicz, 2020a) based architectures were trained on the data to compare the performance of different networks for classification, both with and without preprocessing, with classification perfor-

[7] https://github.com/zeyus/dn3

Figure 7:

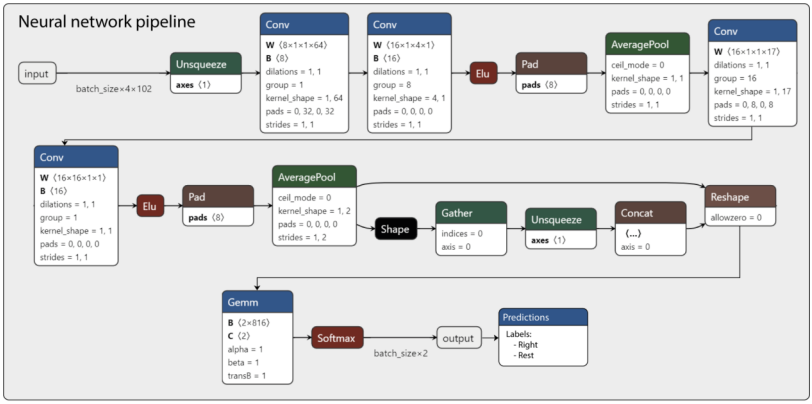

Note. *Overview of the EEGNet based neural network pipeline used for MI classification.*

Figure 8:

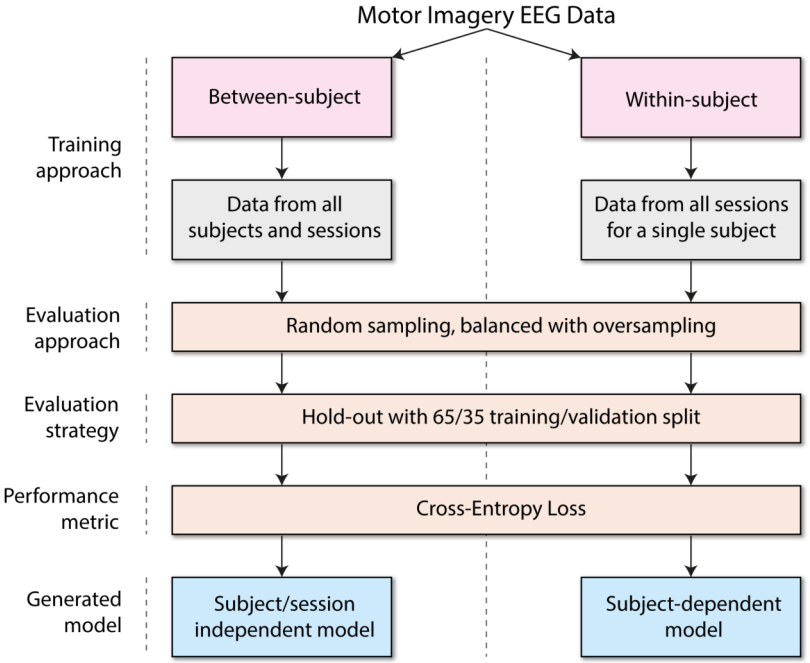

Note. *Diagram describing the process of model training and evaluation.*

mance barely exceeding random chance level.

Although online classification is only viable with a high performing model, due to our goal of making a sub-second MI classifier we implemented an online real-time inference pipeline to assess latency and feasibility. The EEGNet model used resulted in 1 954 trainable parameters (in contrast the BENDR model had 58 284 091 trainable parameters and TIDNet, 608 818 trainable parameters), this reduced number of parameters along with high classification accuracy in benchmarks makes it an ideal architecture for targeting consumer devices which most likely do not have a dedicated GPU/TPU and large amounts of RAM. Minimum continuous latency of [window size] + 205 ms (latency overhead from data transmission, inference, and preprocessing) was consistently achieved with a sliding window step size of 1 sample (meaning 128 predictions/s at 128 Hz sampling rate) on an Intel Core i5-4690K CPU @ 3.50 GHz. These results indicate that online, real-time classification is possible with consumer devices, and finding the narrowest window that maintains high classification accuracy further reduces latency. In our design, the overhead meant that to achieve sub-second online inference, the maximum classification window [window size] was restricted to 0.795 s. This study investigates an even narrower, 0.5 s temporal window for the purposes of classifying motor imagery.

Validation of the network

Prior to testing the capacity of the neural network to predict motor imagery vs. rest behaviours with sub-second latency, the network's baseline prediction capability was tested on data epoched using a 2 s temporal window and compared to the performance of an existing MI-EEG BCI. Yohanandan et al. (2018) reported a mean classification accuracy of 71.09% across 7 participants using a 2 second temporal window, their neural network achieved a mean 63.34% perfor-

mance across 2 participants using 2 s temporal window. Whilst the accuracy achieved here is lower, Yohanandan et al. (2018) used twice the amount of sensors and a sophisticated neurofeedback routine to improve the capability of participants to perform detectable imaginary movements. Thus, our EEGNet network's prediction capability was deemed acceptable for investigating the ability to classify motor imagery using a 0.785 s temporal window.

Results

Table 2:

Parameter	Value
Dropout Probability	0.25
L2 weight decay	0.01
Base learning rate	0.01
Batch size	16
Epochs	500
Kernel size	32
Spatial filters per temporal convolution (D)	2
Temporal filters (F1)	8
Pointwise filters (F2)	16
Pooling	2

Note. *Best performing hyperparameters for both within- and between-subject models*

Classification accuracies for a 0.5 second temporal window for the two participants were 54.8% and 57.1% respectively for subject-dependent models, and 54.1% for the subject-independent model.

Discussion

Motor imagery-based brain computer interfaces hold great promise for enabling individuals with impaired function, diagnosed with conditions such as ALS (Hosni et al., 2020), cerebral palsy (Taherian et al., 2017), or muscular dystrophy (Bao et al., 2021) to interact with the world around them. In contrast with other BCI paradigms, these systems do not rely on external stimulation, but rather on detecting neural activity produced by the user at will, making them easier to use for prolonged periods of time and easier to set-up. While classification accuracy is clearly important, a survey carried out by (Huggins et al., 2015) shows that speed and ease of use are as important for patients interested in using BCI systems.

In this work, we evaluated the possibility of using a practical EEG for real-time classification of rest vs. motor imagery movements with sub-second latency. The data were collected using a low-cost, dry-electrode Ultracortex Mark IV Headset by OpenBCI. The setup of this EEG device does not require expert assistance, making it suitable for at-home use. A lightweight, deep neural network was constructed using EEGNet, a popular compact convolutional neural network for EEG-based brain-computer interfaces. The built system was able to return predictions in real-time with less than a 1–second delay, but the capacity of the classifier to predict events with high accuracy was not achieved. Since the data were acquired in a naturalistic, interference-prone environment, this study also showcases the potential for the proposed BCI system as a robust solution.

Whilst the visual inspection of the signal hinted at the possibility of differentiating between rest vs. MI conditions using a sub-second

temporal window, the neural network could not consistently distinguish the behaviours. As the plots of the signal were taken from a single session, the cause might be the variability between sessions, which was previously reported in other works (Altaheri et al., 2021).

Additional improvements to classification accuracy could be achieved via a denser sensor coverage of the sensory-motor cortex. Most MI-EEG BCI studies utilize data from over 8 electrodes for classification purposes (Altaheri et al., 2021). This study used signals recorded from C3, C4, P3, and P4 electrodes, alternatively, Cz, CP1, CP2, CP5, and CP6 electrodes could be directly added to the Ultracortex Mark IV Headset used in this study.

Limitations and future work

One obvious limitation of the study was its small sample size of two participants, which is not enough to reliably determine whether the proposed approach would generalize to larger populations. Training the neural network on more within-subject and between-subject data would give the network a broader range of activity to pick out the most relevant features of the signal and to give less weight to noise that is less consistent across trials.

Another obvious limitation that needs to be addressed is the low accuracy of the classifier. In a real-world scenario, this can lead to misinterpretation of user intentions, leading to incorrect responses from the system and a decrease in user satisfaction, as well as an increased risk of errors that could be potentially dangerous for the user.

In the section above, the possibility of adding additional sensors with the purpose of covering the sensorimotor cortex more densely was discussed. However, the 3D printed headset by OpenBCI used in the study could not facilitate the addition of the following channels: C1, C2, CP3, CP4, and CPz, which could enhance the targeted ERD/

ERS signal in the acquired data. An alternative headset could be designed and developed for the sole purpose of MI classification, which would include sockets for the sensors listed above. Such additions could increase the network classification accuracy by providing more relevant data.

An attempt at improving classification accuracy could be made via moving the temporal window forward in increments, up to around 0.4 s after the stimulus onset. As seen in Figure 5, when the experimental protocol included a clench condition, the EMG activity did not increase up until around 0.4 s after the stimulus onset, meaning it took approximately 0.4 s for participants to process the stimulus, start acting on it, and subsequently move their muscles. It can be therefore assumed there might also be a delay in the MI condition, minus the latency of signal propagation from the brain to the hand.

The session-dependent variability could be addressed via more consistent performance of the kinesthetic imagery of the required movement. Previous studies on motor imagery have utilized the KVIQ-10 questionnaire (Malouin et al., 2007) to ensure that participants are able to perform the task correctly and consistently, with experimenters explaining and showing the movements prior to the assessment. Alternatively, a neurofeedback training routine akin to that described by Hwang et al., 2009 could be implemented to help participants accurately and consistently perform imaginary movements by presenting them with real-time brain activation graphs.

Whilst this study implemented a visual diagnostic of EMG activity across the two conditions to ensure no muscle activation was present during imaginary movements, a more rigorous and automatic rejection procedure on a per-trial basis could be implemented akin to that by Peterson et al. (2022). This would further ensure that the signal in acquired data is evoked by purely imaginary behaviour, allow-

ing for fewer false positives in the case where the user would clench their right hand.

MI classification in non-stationary settings

As noted at the beginning of the paper, for BCIs to be of value to a larger audience, they need to be usable in non-stationary scenarios. EEG has been proven effective in the classification of multiple types of signals with a high temporal resolution. Unfortunately, it suffers from a high degree of immobility. Motion-related artifacts are one of the most common causes of noise in EEG data. Two other, relatively recently developed methods, namely functional near-infrared spectroscopy (fNIRS) and optically-pumped magnetometers for magnetoencephalography (OPM-MEG) are perfectly suited to tackle this problem. Although fNIRS has a relatively low degree of immobility, its temporal resolution is rather low, meaning that high online classification speed will be difficult to achieve due to the limitations of the technology behind the method. OPM-MEG, however, has an excellent temporal resolution, and benefits from better spatial resolution than EEG, but is more costly (Boto et al., 2016). Importantly, studies have shown OPM-MEG to reliably record neural activity from moving individuals (Boto et al., 2018). Thus, research on the classification capacity of motor imagery in non-stationary settings using OPM-MEG is deemed promising.

Conclusion

This study demonstrated a successful implementation of an EEG-based BCI system able to perform real-time, binary motor imagery classification with a sub-second prediction latency. A low-cost EEG device from OpenBCI was used on data that were acquired in an interference-prone environment, indicating the deployability of the system for real-world applications. Sub-second prediction latency

was achieved using a light CNN based on EEGNet, minimum preprocessing of the raw EEG data, and a temporal window of 0.785 s from the onset of the stimulus. The predictability of motor imagery vs. rest behaviours using a temporal window of 0.785 s was examined. Subject-dependent classification accuracies were 54.8% and 57.1% for the two participants, respectively. Cross-subject classification accuracy was 54.1%. Future work includes evaluating the system using data from more sensors and from participants trained in motor imagery by means of neurofeedback or expert training.

References

Abdi, H., & Williams, L.J. (2010). Principal component analysis: Principal component analysis. *Wiley Interdisciplinary Reviews: Computational Statistics, 2(4),* 433–459. https://doi.org/10.1002/wics.101

Abiri, R., Borhani, S., Sellers, E.W., Jiang, Y., & Zhao, X. (2019). A comprehensive review of EEG-based brain–computer interface paradigms. *Journal of Neural Engineering, 16(1),* 011001. https://doi.org/10.1088/1741-2552/aaf12e

Acharya, U.R., Oh, S.L., Hagiwara, Y., Tan, J.H., Adeli, H., & Subha, D.P. (2018). Automated EEG-based screening of depression using deep convolutional neural network. *Computer Methods and Programs in Biomedicine, 161,* 103–113. https://doi.org/10.1016/j.cmpb.2018.04.012

Altaheri, H., Muhammad, G., Alsulaiman, M., Amin, S.U., Altuwaijri, G.A., Abdul, W., Bencherif, M.A., & Faisal, M. (2021). Deep learning techniques for classification of electroencephalogram (EEG) motor imagery (MI) signals: A review. Neural Computing and Applications. https://doi.org/10.1007/s00521-021-06352-5

An, X., Kuang, D., Guo, X., Zhao, Y., & He, L. (2014). A Deep Learning Method for Classification of EEG Data Based on Motor Imagery. In D.-S. Huang, K. Han, & M. Gromiha (Eds.), Intelligent Computing in Bioinformatics (Vol. 8590, pp. 203–210). Springer International Publishing. https://doi.org/10.1007/978-3-319-09330-7_25

Artola, A., Bröcher, S., & Singer, W. (1990). Different voltage-dependent thresholds for inducing long-term depression and long-term potentiation in slices of rat visual cortex. *Nature, 347(6288),* 69–72. https://doi.org/10.1038/347069a0

Ball, T., Kern, M., Mutschler, I., Aertsen, A., & Schulze-Bonhage, A. (2009). Signal quality of simultaneously recorded invasive and non-invasive EEG. *NeuroImage, 46(3),* 708–716. https://doi.org/10.1016/j.neuroimage.2009.02.028

Bao, S.-C., Yuan, K., Chen, C., Lau, C.C., & Tong, R.K. (2021). A Motor Imagery-based Brain-Computer Interface Scheme for a Spinal Muscular Atrophy Subject in CYBATHLON Race. *2021 10th International IEEE/EMBS Conference on Neural Engineering (NER),* 532–535. https://doi.org/10.1109/NER49283.2021.9441351

Barsotti, M., Leonardis, D., Loconsole, C., Solazzi, M., Sotgiu, E., Procopio, C., Chisari,C., Bergamasco, M., & Frisoli, A. (2015). A full upper limb robotic exoskeleton for reaching and grasping rehabilitation triggered by MI-BCI. *2015 IEEE International Conference on Rehabilitation Robotics (ICORR),* 49–54. https://doi.org/10.1109/ICORR.2015.7281174

Bliss, T.V.P., & Lømo, T. (1973). Long-lasting potentiation of synaptic transmission in the dentate area of the anaesthetized rabbit following stimulation of the perforant path. *The Journal of Physiology, 232(2),* 331–356. https://doi.org/10.1113/jphysiol.1973.sp010273

Bojarski, M., Del Testa, D., Dworakowski, D., Firner, B., Flepp, B., Goyal, P., Jackel, L.D., Monfort, M., Muller, U., Zhang, J., Zhang, X., Zhao, J., & Zieba, K. (2016). End to End Learning for Self-Driving Cars. https://doi.org/10.48550/ARXIV.1604.07316

Boto, E., Bowtell, R., Krüger, P., Fromhold, T.M., Morris, P.G., Meyer, S.S., Barnes, G.R., & Brookes, M.J. (2016). On the Potential of a New Generation of Magnetometers for MEG: A Beamformer Simulation Study. *PLOS ONE, 11(8),* e0157655. https://doi.org/10.1371/journal.pone.0157655

Boto, E., Holmes, N., Leggett, J., Roberts, G., Shah, V., Meyer, S.S., Muñoz, L.D., Mullinger, K.J., Tierney, T.M., Bestmann, S., Barnes, G.R., Bowtell, R., & Brookes, M.J. (2018). Moving magnetoencephalography towards real-world applications with a wearable system. *Nature, 555(7698),* 657–661. https://doi.org/10.1038/nature26147

Cecotti, H., & Graser, A. (2010). Convolutional Neural Networks for P300 Detection with Application to Brain-Computer Interfaces. IEEE.

Chang, M.H., Baek, H.J., Lee, S.M., & Park, K.S. (2014). An amplitude-modulated visual stimulation for reducing eye fatigue in SSVEP-based brain–computer interfaces. *Clinical Neurophysiology, 125(7),* 1380–1391. https://doi.org/10.1016/j.clinph.2013.11.016

Christensen, S.M., Holm, N.S., & Puthusserypady, S. (2019). An Improved Five Class MI Based BCI Scheme for Drone Control Using Filter Bank CSP. *2019 7th International Winter Conference on Brain-Computer Interface (BCI),* 1–6. https://doi.org/10.1109/IWW-BCI.2019.8737263

Craik, A., He, Y., & Contreras-Vidal, J.L. (2019). Deep learning for electroencephalogram (EEG) classification tasks: A review. *Journal of Neural Engineering, 16(3),* 031001. https://doi.org/10.1088/1741-2552/ab0ab5

Dickstein, R., & Deutsch, J.E. (2007). Motor Imagery in Physical Therapist Practice. *Physical Therapy, 87(7),* 942–953. https://doi.org/10.2522/ptj.20060331

Fabiani, M., Gratton, G., Karis, D., & Donchin, E. (1987). Definition, identification, and reliability of measurement of the P300 component of the event-related brain potential. *Advances in Psychophysiology, 2(S1),* 78.

Farwell, L.A., & Donchin, E. (1988). Talking off the top of your head: Toward a mental prosthesis utilizing event-related brain potentials. *Electroencephalography and Clinical Neurophysiology, 70(6),* 510–523. https://doi.org/10.1016/0013-4694(88)90149-6

Friston, K.J. (2009). Modalities, Modes, and Models in Functional Neuroimaging. *Science, 326(5951),* 399–403. https://

doi.org/10.1126/science.1174521

Guger, C., Ramoser, H., & Pfurtscheller, G. (2000). Real-time EEG analysis with subject-specific spatial patterns for a brain-computer interface (BCI). *IEEE Transactions on Rehabilitation Engineering, 8(4),* 447–456. https://doi.org/10.1109/86.895947

Hebb, D.O. (1949). The Organization of Behaviour.

Hosni, S.M., Borgheai, S.B., McLinden, J., & Shahriari, Y. (2020). An fNIRS-Based Motor Imagery BCI for ALS: A Subject-Specific Data-Driven Approach. *IEEE Transactions on Neural Systems and Rehabilitation Engineering, 28(12),* 3063–3073. https://doi.org/10.1109/TNSRE.2020.3038717

Huggins, J.E., Moinuddin, A.A., Chiodo, A.E., & Wren, P.A. (2015). What Would Brain-Computer Interface Users Want: Opinions and Priorities of Potential Users With Spinal Cord Injury. *Archives of Physical Medicine and Rehabilitation, 96(3),* S38-S45.e5. https://doi.org/10.1016/j.apmr.2014.05.028

Hussein, R., Palangi, H., Ward, R.K., & Wang, Z.J. (2019). Optimized deep neural network architecture for robust detection of epileptic seizures using EEG signals. *Clinical Neurophysiology, 130(1),* 25–37. https://doi.org/10.1016/j.clinph.2018.10.010

Hwang, H.-J., Han, C.-H., Lim, J.-H., Kim, Y.-W., Choi, S.-I., An, K.-O., Lee, J.-H., Cha, H.-S., Hyun Kim, S., & Im, C.-H. (2017). Clinical feasibility of brain-computer interface based on steady-state visual evoked potential in patients with locked-in syndrome: Case studies: Clinical feasibility of SSVEP-based BCI. *Psychophysiology, 54(3),* 444–451. https://doi.org/10.1111/psyp.12793

Hwang, H.-J., Kwon, K., & Im, C.-H. (2009). Neurofeedback-based motor imagery training for brain–computer interface (BCI). *Journal of Neuroscience Methods, 179(1),* 150–156. https://doi.org/10.1016/j.jneumeth.2009.01.015

Jeannerod, M. (1995). Mental imagery in the motor context. *Neuropsychologia, 33(11),* 1419–1432. https://doi.org/10.1016/0028-3932(95)00073-C

Kevric, J., & Subasi, A. (2017). Comparison of signal decomposition methods in classification of EEG signals for motor-imagery BCI system. *Biomedical Signal Processing and Control, 31,* 398–406. https://doi.org/10.1016/j.bspc.2016.09.007

Khan, M.J., & Hong, K.-S. (2015). Passive BCI based on drowsiness detection: An fNIRS study. *Biomedical Optics Express, 6(10),* 4063. https://doi.org/10.1364/BOE.6.004063

Khosla, A., Khandnor, P., & Chand, T. (2020). A comparative analysis of signal processing and classification methods for different applications based on EEG signals. *Biocybernetics and Biomedical Engineering, 40(2),* 649–690. https://doi.org/10.1016/j.bbe.2020.02.002

Kirschstein, T., & Köhling, R. (2009). What is the Source of the EEG? *Clinical EEG and Neuroscience, 40(3),* 146–149. https://doi.org/10.1177/155005940904000305

Kostas, D., Aroca-Ouellette, S., & Rudzicz, F. (2021). BENDR: Using Transformers and a Contrastive Self-Supervised Learning Task to Learn From Massive Amounts of EEG Data. *Frontiers in Human Neuroscience, 15,* 653659. https://doi.org/10.3389/fnhum.2021.653659

Kostas, D., & Rudzicz, F. (2020a). Thinker invariance: Enabling deep neural networks for BCI across more people. *Journal of Neural Engineering, 17(5),* 056008. https://doi.org/10.1088/1741-2552/abb7a7

Kostas, D., & Rudzicz, F. (2020b). DN3: An open-source Python library for large-scale raw neurophysiology data assimilation for more flexible and standardized deep learning [Preprint]. *Neuroscience.* https://doi.org/10.1101/2020.12.17.423197

Kraeutner, S., Gionfriddo, A., Bardouille, T., & Boe, S. (2014). Motor imagery-based brain activity parallels that of motor execution: Evidence from magnetic source imaging of cortical oscillations. *Brain Research, 1588,* 81–91. https://doi.org/10.1016/j.brainres.2014.09.001

Krizhevsky, A., Sutskever, I., & Hinton, G.E. (2012). ImageNet Classification with Deep Convolutional Neural Networks. In F. Pereira, C. J. Burges, L. Bottou, & K. Q. Weinberger (Eds.), Advances in Neural Information Processing Systems (Vol. 25). Curran Associates, Inc. https://proceedings.neurips.cc/paper/2012/file/c399862d3b9d6b76c8436e924a68c45b-Paper.pdf

Krusienski, D.J., Sellers, E.W., McFarland, D.J., Vaughan, T.M., & Wolpaw, J.R. (2008). Toward enhanced P300 speller performance. *Journal of Neuroscience Methods, 167(1),* 15–21. https://doi.org/10.1016/j.jneumeth.2007.07.017

Kuś, R., Duszyk, A., Milanowski, P., Łabęcki, M., Bierzyńska, M., Radzikowska, Z., Michalska, M., Żygierewicz, J., Suffczyński, P., & Durka, P.J. (2013). On the Quantification of SSVEP Frequency Responses in Human EEG in Realistic BCI Conditions. *PLoS ONE, 8(10),* e77536. https://doi.org/10.1371/journal.pone.0077536

Kwak, N.-S., Müller, K.-R., & Lee, S.-W. (2015). A lower limb exoskeleton control system based on steady state visual evoked potentials. *Journal of Neural Engineering, 12(5),* 056009. https://doi.org/10.1088/1741-2560/12/5/056009

Lawhern, V.J., Solon, A.J., Waytowich, N.R., Gordon, S.M., Hung, C.P., & Lance, B.J. (2018). EEGNet: A compact convolutional neural network for EEG-based brain–computer interfaces. *Journal of Neural Engineering, 15(5),* 056013. https://doi.org/10.1088/1741-2552/aace8c

Lebedev, M.A., & Nicolelis, M.A.L. (2017). Brain-Machine Interfaces: From Basic Science to Neuroprostheses and Neuroreha-

bilitation. *Physiological Reviews, 97(2),* 767–837. https://doi.org/10.1152/physrev.00027.2016

Lotze, M., & Halsband, U. (2006). Motor imagery. *Journal of Physiology-Paris, 99(4–6),* 386–395. https://doi.org/10.1016/j.jphysparis.2006.03.012

Lun, X., Yu, Z., Chen, T., Wang, F., & Hou, Y. (2020). A Simplified CNN Classification Method for MI-EEG via the Electrode Pairs Signals. *Frontiers in Human Neuroscience, 14,* 338. https://doi.org/10.3389/fnhum.2020.00338

Ma, X., Qiu, S., & He, H. (2020). Multi-channel EEG recording during motor imagery of different joints from the same limb. *Scientific Data, 7(1),* 191. https://doi.org/10.1038/s41597-020-0535-2

Malouin, F., Jackson, P.L., & Richards, C.L. (2013). Towards the integration of mental practice in rehabilitation programs. A critical review. *Frontiers in Human Neuroscience*, 7. https://doi.org/10.3389/fnhum.2013.00576

Malouin, F., Richards, C.L., Jackson, P.L., Lafleur, M.F., Durand, A., & Doyon, J. (2007). The Kinesthetic and Visual Imagery Questionnaire (KVIQ) for Assessing Motor Imagery in Persons with Physical Disabilities: A Reliability and Construct Validity Study. *Journal of Neurologic Physical Therapy, 31(1),* 20–29. https://doi.org/10.1097/01.NPT.0000260567.24122.64

McCrimmon, C.M., Wang, M., Lopes, L.S., Wang, P.T., Karimi-Bidhendi, A., Liu, C.Y., Heydari, P., Nenadic, Z., & Do, A.H. (2016). A small, portable, battery-powered brain-computer interface system for motor rehabilitation. *2016 38th Annual International Conference of the IEEE Engineering in Medicine and Biology Society (EMBC),* 2776–2779. https://doi.org/10.1109/EMBC.2016.7591306

McFarland, D.J., & Vaughan, T.M. (2016). BCI in practice. *In Progress in Brain Research (Vol. 228, pp. 389–404).* Elsevier. https://doi.org/10.1016/bs.pbr.2016.06.005

Morabito, F.C., Campolo, M., Ieracitano, C., Ebadi, J.M., Bonanno, L., Bramanti, A., Desalvo, S., Mammone, N., & Bramanti, P. (2016). Deep convolutional neural networks for classification of mild cognitive impaired and Alzheimer's disease patients from scalp EEG recordings. *2016 IEEE 2nd International Forum on Research and Technologies for Society and Industry Leveraging a Better Tomorrow (RTSI),* 1–6. https://doi.org/10.1109/RTSI.2016.7740576

Newell, K.M. (1991). Motor skill acquisition. Annual Review of Psychology, 42(1), 213-237. Nutt, R. (2002). The History of Positron Emission Tomography. *Molecular Imaging & Biology, 4(1),* 11–26. https://doi.org/10.1016/S1095-0397(00)00051-0

Olejniczak, P. (2006). Neurophysiologic Basis of EEG: *Journal of Clinical Neurophysiology, 23(3),* 186–189. https://doi.org/10.1097/01.wnp.0000220079.61973.6c

ONNX Runtime developers. (2021). ONNX Runtime. https://onnxruntime.ai/

Paek, A.Y., Kilicarslan, A., Korenko, B., Gerginov, V., Knappe, S., & Contreras-Vidal, J.L. (2020). Towards a Portable Magnetoencephalography Based Brain Computer Interface with Optically-Pumped Magnetometers. 2020 *42nd Annual International Conference of the IEEE Engineering in Medicine & Biology Society (EMBC),* 3420–3423. https://doi.org/10.1109/EMBC44109.2020.9176159

Peirce, J., Gray, J.R., Simpson, S., MacAskill, M., H"ochenberger, R., Sogo, H., Lindelov, J.S. (2019). PsychoPy2: Experiments in behavior made easy. *Behavior Research Methods, 51(1),* 195–203. https://doi.org/10.3758/s13428-018-01193-y

Peterson, V., Galván, C., Hernández, H., Saavedra, M.P., & Spies, R. (2022). A motor imagery vs. Rest dataset with low-cost consumer grade EEG hardware. *Data in Brief, 42,* 108225. https://doi.org/10.1016/j.dib.2022.108225

Pfurtscheller, G. (2000). Chapter 26 Spatiotemporal ERD/ERS patterns during voluntary movement and motor imagery. *In Supplements to Clinical Neurophysiology (Vol. 53, pp. 196–198).* Elsevier. https://doi.org/10.1016/S1567-424X(09)70157-6

Pfurtscheller, G., & Neuper, C. (1997). Motor imagery activates primary sensorimotor area in humans. *Neuroscience Letters, 239(2–3),* 65–68. https://doi.org/10.1016/S0304-3940(97)00889-6

Pfurtscheller, G., Solis-Escalante, T., Ortner, R., Linortner, P., & Muller-Putz, G.R. (2010). Self-Paced Operation of an SSVEP-Based Orthosis With and Without an Imagery-Based "Brain Switch:" A Feasibility Study Towards a Hybrid BCI. *IEEE Transactions on Neural Systems and Rehabilitation Engineering, 18(4),* 409–414. https://doi.org/10.1109/TNSRE.2010.2040837

Pichiorri, F., & Mattia, D. (2020). Brain-computer interfaces in neurologic rehabilitation practice. *In Handbook of Clinical Neurology (Vol. 168, pp. 101–116).* Elsevier. https://doi.org/10.1016/B978-0-444-63934-9.00009-3

Rebsamen, B., Burdet, E., Guan, C., Zhang, H., Teo, C.L., Zeng, Q., Laugier, C., & Ang, M.H. (2007). Controlling a Wheelchair Indoors Using Thought. *IEEE Intelligent Systems, 22(2),* 18–24. https://doi.org/10.1109/MIS.2007.26

Reshmi, G., & Amal, A. (2013). Design of a BCI System for Piloting a Wheelchair Using Five Class MI Based EEG. *2013 Third International Conference on Advances in Computing and Communications,* 25–28. https://doi.org/10.1109/ICACC.2013.12

Robertson, E.M., Pascual-Leone, A., & Miall, R.C. (2004). Current concepts in procedural consolidation. *Nature Reviews Neuroscience, 5(7),* 576–582. https://doi.org/10.1038/nrn1426

Schalk, G. (2009). Sensor Modalities for Brain-Computer Interfacing. In J. A. Jacko (Ed.), Human-Computer Interaction. *Novel Interaction Methods and Techniques (Vol. 5611, pp. 616–622).* Springer Berlin Heidelberg. https://doi.org/10.1007/978-3-

642-02577-8_67

Schalk, G., & Leuthardt, E.C. (2011). Brain-Computer Interfaces Using Electrocorticographic Signals. *IEEE Reviews in Biomedical Engineering, 4,* 140–154. https://doi.org/10.1109/RBME.2011.2172408

Schuster, C., Hilfiker, R., Amft, O., Scheidhauer, A., Andrews, B., Butler, J., Kischka, U., & Ettlin, T. (2011). Best practice for motor imagery: A systematic literature review on motor imagery training elements in five different disciplines. *BMC Medicine, 9(1),* 75. https://doi.org/10.1186/1741-7015-9-75

Gao, S.,Shangkai Gao, Wang, Y.,Yijun Wang, Gao, X., Xiaorong Gao, & Hong, B.Bo Hong. (2014). Visual and Auditory Brain–Computer Interfaces. *IEEE Transactions on Biomedical Engineering, 61(5),* 1436–1447. https://doi.org/10.1109/TBME.2014.2300164

Sitaram, R., Caria, A., Veit, R., Gaber, T., Rota, G., Kuebler, A., & Birbaumer, N. (2007). fMRI Brain-Computer Interface: A Tool for Neuroscientific Research and Treatment. *Computational Intelligence and Neuroscience, 2007,* 1–10. https://doi.org/10.1155/2007/25487

Stinear, C.M., Byblow, W.D., Steyvers, M., Levin, O., & Swinnen, S.P. (2006). Kinesthetic, but not visual, motor imagery modulates corticomotor excitability. *Experimental Brain Research, 168(1–2),* 157–164. https://doi.org/10.1007/s00221-005-0078-y

Stone, J. V. (2002). Independent component analysis: An introduction. *Trends in Cognitive Sciences, 6(2),* 59–64. https://doi.org/10.1016/S1364-6613(00)01813-1

Tabar, Y.R., & Halici, U. (2017). A novel deep learning approach for classification of EEG motor imagery signals. *Journal of Neural Engineering, 14(1),* 016003. https://doi.org/10.1088/1741-2560/14/1/016003

Taherian, S., Selitskiy, D., Pau, J., & Claire Davies, T. (2017). Are we there yet? Evaluating commercial grade brain–computer interface for control of computer applications by individuals with cerebral palsy. *Disability and Rehabilitation: Assistive Technology, 12(2),* 165–174. https://doi.org/10.3109/17483107.2015.1111943

Tanner, D., Morgan-Short, K., & Luck, S.J. (2015). How inappropriate high-pass filters can produce artifactual effects and incorrect conclusions in ERP studies of language and cognition: High-pass filtering and artifactual ERP effects. *Psychophysiology, 52(8),* 997–1009. https://doi.org/10.1111/psyp.12437

Vaughan, T.M., McFarland, D.J., Schalk, G., Sarnacki, W.A., Krusienski, D.J., Sellers, E.W., & Wolpaw, J.R. (2006). The wadsworth BCI research and development program: At home with BCI. *IEEE Transactions on Neural Systems and Rehabilitation Engineering, 14(2),* 229–233. https://doi.org/10.1109/TNSRE.2006.875577

Vialatte, F.-B., Maurice, M., Dauwels, J., & Cichocki, A. (2010). Steady-state visually evoked potentials: Focus on essential paradigms and future perspectives. *Progress in Neurobiology, 90(4),* 418–438. https://doi.org/10.1016/j.pneurobio.2009.11.005

Willett, F.R., Avansino, D.T., Hochberg, L.R., Henderson, J.M., & Shenoy, K.V. (2021). High-performance brain-to-text communication via handwriting. *Nature, 593(7858),* 249–254. https://doi.org/10.1038/s41586-021-03506-2

Yang, J., Ma, Z., Wang, J., & Fu, Y. (2020). A Novel Deep Learning Scheme for Motor Imagery EEG Decoding Based on Spatial Representation Fusion. *IEEE Access, 8,* 202100–202110. https://doi.org/10.1109/ACCESS.2020.3035347

Yao, L., Sheng, X., Zhang, D., Jiang, N., Farina, D., & Zhu, X. (2017). A BCI System Based on Somatosensory Attentional Orientation. *IEEE Transactions on Neural Systems and Rehabilitation Engineering, 25(1),* 81–90. https://doi.org/10.1109/TNSRE.2016.2572226

Yohanandan, S.A. C., Kiral-Kornek, I., Tang, J., Mshford, B. S., Asif, U., & Harrer, S. (2018). A Robust Low-Cost EEG Motor Imagery-Based Brain-Computer Interface. *2018 40th Annual International Conference of the IEEE Engineering in Medicine and Biology Society (EMBC),* 5089–5092. https://doi.org/10.1109/EMBC.2018.8513429

Zhang, K., Robinson, N., Lee, S.-W., & Guan, C. (2021). Adaptive transfer learning for EEG motor imagery classification with deep Convolutional Neural Network. *Neural Networks, 136,* 1–10. https://doi.org/10.1016/j.neunet.2020.12.013